In-situ crystal structure determination of seifertite SiO$_2$ at 129 GPa: Studying a minor phase near Earth's core–mantle boundary ⚐

LI ZHANG[1,*], DMITRY POPOV[2], YUE MENG[2], JUNYUE WANG[1,3], CHENG JI[1,4], BING LI[1,4] AND HO-KWANG MAO[1,3]

[1]Center for High Pressure Science and Technology Advanced Research (HPSTAR), Shanghai 201203, China
[2]High Pressure Collaborative Access Team (HPCAT), Geophysical Laboratory, Carnegie Institution of Washington, Argonne, Illinois 60439, U.S.A.
[3]Geophysical Laboratory, Carnegie Institution of Washington, Washington, D.C. 20015, U.S.A.
[4]High Pressure Synergetic Consortium (HPSynC), Geophysical Laboratory, Carnegie Institution of Washington, Argonne, Illinois 60439, U.S.A.

ABSTRACT

Seifertite SiO$_2$ likely exists as a minor phase near the core–mantle boundary. By simulating the pressure and temperature conditions near the core–mantle boundary, seifertite was synthesized as a minor phase in a coarse-grained, polycrystalline sample coexisting with the (Mg,Fe)SiO$_3$ post-perovskite (pPv) phase at 129 GPa and 2500 K. Here we report the first in situ single-crystal structure determination and refinement of seifertite at high pressure and after a temperature quench from laser heating. We improved the data coverage of a minor phase from a diamond-anvil cell (DAC) by merging single-crystal data of seifertite from six selected grains that had different orientations. Observed systematic absences of reflections from the six individual grains allowed only one space group: *Pbcn*. The refined results of seifertite are in good agreement with the predictions from previous first-principles calculations at high pressure. This approach provides a method for structure determination of a minor phase in a mineral assemblage synthesized under *P-T* conditions representative of the deep Earth.

Keywords: High pressure, crystal structure, multigrain, SiO$_2$, seifertite, synchrotron X-ray, deep mantle

INTRODUCTION

Earth's core–mantle boundary (CMB) is located at approximately 2900 km beneath the surface, corresponding to pressures (*P*) of 136 GPa and temperatures (*T*) greater than 2500 K. SiO$_2$ is a common mineral in the Earth's crust, and silicates comprise most of the mantle. Free SiO$_2$ may also exist as a minor phase in the mantle through subduction of mid-ocean ridge basalt (MORB) crust (Andrault et al. 2014; Hirose et al. 2005). Under *P* and *T* conditions relevant to the Earth's lower mantle, SiO$_2$ transforms from stishovite to CaCl$_2$-type at ~50 GPa and room temperature (Cohen 1992; Kingma et al. 1994), then to α-PbO$_2$ like structure known as seifertite (El Goresy et al. 2008) at *P-T* conditions near the CMB (Dubrovinsky et al. 1997; Grocholski et al. 2013). Knowing the accurate crystal structure of seifertite at relevant *P-T* conditions is fundamentally important for understanding the deep mantle.

The space group of seifertite has been under debate due to the similarity of the systematic absences of several space groups (Belonoshko et al. 1996; Dera et al. 2002; Dubrovinsky et al. 1997; Karki et al. 1997a, 1997b; Teter et al. 1998; Tse et al. 1992; Tsuchida and Yagi 1990). When the phase was first experimentally discovered in a DAC (Dubrovinsky et al. 1997), the few peaks observed in the powder XRD pattern did not allow an unambiguous structure determination, and thus the study assumed the theoretical predication of space group *Pnc*2 (Belonoshko et al. 1996). A post-stishovite phase of SiO$_2$ was also discovered in the Shergotty Meteorite (Sharp et al. 1999), and the powder X-ray diffraction (XRD) data of this meteorite sample suggested the space group *Pbcn* (Dera et al. 2002). However, the study also pointed out that the power XRD pattern alone could not unambiguously conclude the centrosymmetric structure (Dera et al. 2002). Later first-principles calculations came to agreement on the space group *Pbcn* (Karki et al. 1997a, 1997b; Teter et al. 1998). To date, however, an unambiguous structure determination of seifertite within its stability field has not yet been achieved, due to the challenges in structure studies at ultrahigh pressure. Seifertite appears as a minor phase in the run product at *P-T* conditions representative of the CMB when MORB or Fe-rich orthopyroxene are used as the starting material, and such sample environments may influence the crystal chemistry of seifertite (Hirose et al. 2005).

STRUCTURE DETERMINATION OF A MINOR PHASE IN A MULTIPHASE ASSEMBLAGE

Powder X-ray diffraction (XRD) in a DAC has intrinsic limitations when the sample consists of multiple phases with low symmetries. Overlapping peaks in such a powder XRD pattern make phase indexation and structure determination challenging in high-pressure studies. On the other hand, single-crystal XRD provides a more definitive characterization of a crystal structure at high pressure. To achieve good coverage of reciprocal space from a single-crystal in a DAC, efforts have been made to maximize the DAC opening while still maintaining high pressure (Boehler 2006). However, even in a successful single-crystal DAC experiment, only a portion of the reciprocal space can be illuminated by X-rays (Miletich et al. 2000). Meanwhile, a single pre-selected crystal (or several) can only be maintained in a soft medium of He or Ne to a certain pressure (~50 GPa). At elevated pressures, preloaded single crystals either become degraded or break into polycrystallites when passing through a phase transition. In addi-

---

tion, multiple phases often coexist in a polycrystalline sample as a result of phase equilibrium in high-pressure petrological studies, and the structure determination and crystal chemistry of each phase is fundamentally important for understanding the phase relations in such systems. However, new structures and minor phases are often overshadowed by the diffraction of major phases in a powder diffraction pattern, and are impossible to identify. Therefore, the structure determination of a minor phase in such a multiphase assemblage at high pressure has never been previously possible using conventional single-crystal or powder diffraction techniques.

Utilization of the multigrain method (Sørensen et al. 2012) for a polycrystalline sample in a DAC has opened a new area for high-pressure crystallography at megabar pressures (Nisr et al. 2012; Zhang et al. 2013). The multigrain approach also allows the separation of crystallographic information of an unknown phase from a mixture at high pressure (Zhang et al. 2014). As the X-ray beams available at synchrotron facilities tend to be very focused and intense, most of the powder XRD patterns will show some degree of spottiness. Heating a powder sample can further promote spottiness in a powder XRD pattern due to crystal growth at high temperature. The multigrain approach shows great advantages for in situ studying of a polycrystalline sample at high pressure by finding an individual orientation matrix for each individual grain, allowing high-pressure crystallographic studies unachievable using conventional single-crystal techniques. In this study, we demonstrate a solution for structure determination of a minor phase in a multiple phase assemblage at conditions representative of the CMB.

SYNTHESIS OF SEIFERTITE AS A MINOR PHASE AND ITS UNIT-CELL PARAMETERS

In this study, an orthopyroxene sample with $(Mg_{0.6}Fe_{0.4})SiO_3$ composition and ~5% excess of SiO_2 was used as the starting material. The starting material was pre-compressed into disks of ~10 μm thickness and cut to ~40 μm in diameter and placed in a rhenium (Re) gasket hole in a Mao-type symmetric DAC filled with Ne. Diamond anvils with flat culet diameters of 120 μm beveled at 10° up to 300 μm were mounted in Boehler seats with 60° X-ray opening. The micro-focused X-ray diffraction with in situ laser heating available at 16IDB at the Advanced Photon Source (APS) of Argonne National Laboratory was used to study changes in the sample at *P-T* conditions representative of the CMB. Temperatures were measured on both sides by spectroradiometry and pressures were determined from the unit-cell volumes of Ne (Fei et al. 2007) after *T* quench.

Seifertite was synthesized at 129 GPa and 2500 K. The unit-cell parameter of Ne after *T* quench was 2.903(8) Å calculated from four diffraction lines 111, 200, 220, and 311. Figures 1a and 1b show seifertite as a minor phase coexisting with pPv and the characteristic peak 110 at 2.90 Å and 111 at 2.39 Å were identified for seifertite. Over 40 000 diffraction spots were obtained from the spotty XRD patterns collected by rotating the DAC from –24 to 24° at steps of 0.2°. Such a small angular step was used to improve the signal-to-noise ratio by reducing the background level. The exposure time was 4 s/frame. The FABLE package (Sørensen et al. 2012) was used to filter the spots, and GrainSpotter (Schmidt 2014) in the package was used to assign the reflections to each of the specific orientation matrices. Over 100 grains were identi-
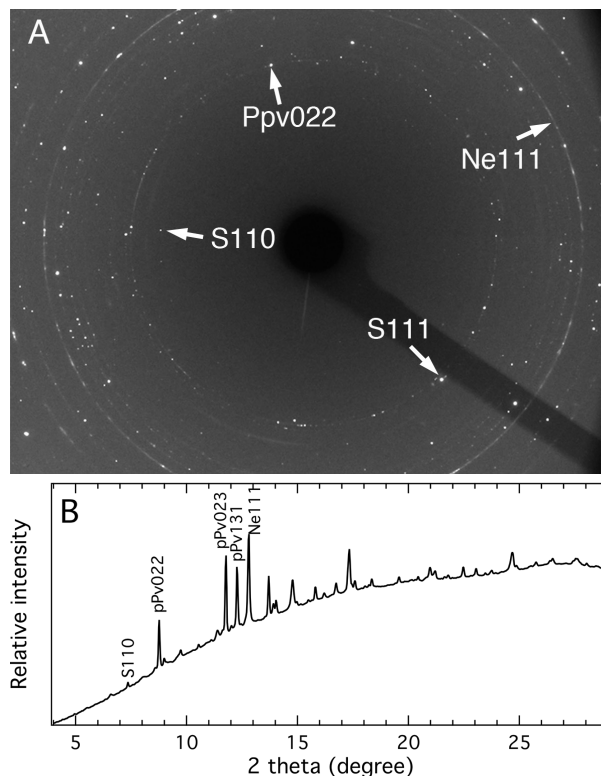

FIGURE 1. XRD data of seifertite at 129 GPa and after *T* quench (X-ray wavelength of 0.3738 Å). (**a**) A representative spotty XRD pattern of seifertite coexisting with the dominant phase pPv at a fixed rotation angle. S = silica, pPv = post-perovskite, Ne = neon. (**b**) An integrated powder pattern at a fixed omega angle showing the intensity contrast between the major phase (Mg,Fe)SiO₃-pPv and seifertite.

fied, but most are too fine for structure analysis. Only six grains with maximum number of reflections were selected for further structure studies.

Multigrain patterns allow separation of reflections with close *d*-spacings and picking up weak reflections. Figure 2 shows three pairs of diffraction reflections from one selected grain of seifertite. In a 2D powder XRD pattern, the {302} diffraction ring with *d*-spacing of 1.067 Å would overlap with {321} with 1.061 Å; in a multigrain pattern, however, each of the reflections can be unambiguously identified through its unique rotation, Bragg and azimuth angles, as shown in Figures 2a and 2b. Additionally, weak diffraction peaks are often overshadowed by the background noise in a smooth powder XRD pattern; in contrast, a couple of diffraction spots contribute to most of the intensity of a diffraction peak in a multigrain pattern, and, therefore, weak reflections, such as the {421} reflections shown in Figure 2c, can be picked out, despite having only a few pixels slightly more intense than the background.

In the powder pattern most peaks at high *d*-spacing were overshadowed by the strong peaks from the major phase pPv as shown in Figure 1b, only one characteristic peak of seifertite (2.90 Å) was visible in the low *d*-spacing region, preventing determination of unit-cell parameters of this orthorhombic phase. On the other hand, the multigrain approach allows us to calculate the unit-cell
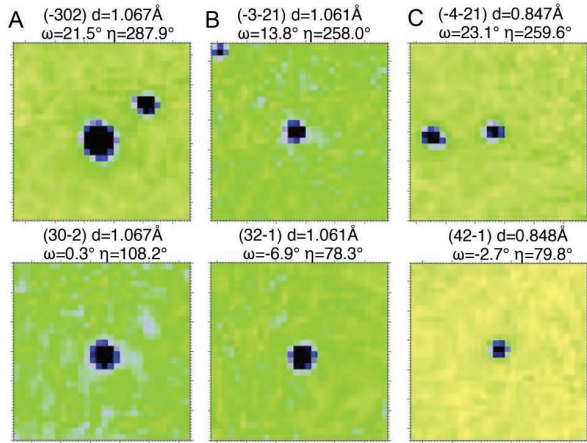
FIGURE 2. Selected diffraction reflections from one grain of seifertite are shown in the middle within 30 × 30 pixels (pixel size: 79 μm) at 129 GPa. (**a–b**) The multigrain method distinguishes a pair of {302} reflections from another pair of {321} with close *d*-spacing. (**c**) A pair of weak {421} reflections with only a few pixels slightly more intense than the background can be picked out by the multigrain method.

TABLE 1. Calculated unit-cell parameters from multiple grains of seifertite at 129 GPa and room *T*

Parameters	Grain1	Grain2	Grain3	Grain4	Grain 1+2	Grain 1+2+3	Grain 1+2+3+4
a (Å)	3.72908	3.72933	3.72762	3.72537	3.72919	3.72862	3.72774
σ(*a*)	0.00040	0.00030	0.00027	0.00027	0.00024	0.00018	0.00015
B (Å)	4.65973	4.65857	4.65534	4.65754	4.65927	4.65765	4.65760
σ(*b*)	0.00051	0.00060	0.00045	0.00054	0.00039	0.00027	0.00024
c (Å)	4.16033	4.15955	4.16708	4.16019	4.15994	4.16076	4.16090
σ(*c*)	0.00048	0.00049	0.00169	0.00083	0.00034	0.00033	0.00030
V (Å³)	72.2920	72.2653	72.3127	72.1839	72.2803	72.2583	72.2429
σ(*V*)	0.0087	0.0095	0.0245	0.0106	0.0063	0.0055	0.0047
N (refl.)	48	48	50	47	96	146	193

parameters from multiple grains through three-dimensional orientation and geometrical relationships. Table 1 shows the calculated unit-cell parameters from four individual grains and merged grains using the software UNITCELL (Holland and Redfern 1997). The unit-cell parameters of seifertite refined from nearly 200 reflections at 129 GPa are: $a = 3.7277(2)$, $b = 4.6576(2)$, $c = 4.1609(3)$, and $V = 72.243(5)$ Å. The uncertainties in *d*-values are mainly defined by resolution of the monochromator. The unit-cell volume obtained in this study is 1.1% higher than the volume from previous powder XRD data at 129 GPa (Grocholski et al. 2013), likely due to the difference between different pressure scales. The *a/b* and *a/c* ratios from another powder XRD study (Murakami 2003) are 3.7 and 1.0% lower than the values obtained from our study, respectively, probably due to the non-hydrostatic environment and the limited number of reflections available for the unit-cell determination in the previous study.

## STRUCTURE DETERMINATION AND REFINEMENT OF SEIFERTITE

Intensities of reflections from each selected grain have been calculated using the XDS software (Kabsch 2010). This program uses very efficient integration and scaling algorithms, but it assumes that reflections from only one crystal are present on X-ray images. That was why, among all the diffraction spots identified by XDS, only those from a selected grain had to be selected. For this purpose indices and coordinates of a pair of reflections identified using the FABLE package were used to calculate the orientation matrix (Busing and Levy 1967), which in turn allowed us to identify all the reflections belonging to this grain. All further data processing by XDS was done as normal, assuming there was only one crystal in the beam. XDS does not allow the definition of shaded areas changing during the data collection routine. Another program was developed to define the shaded areas based on the orientation and opening of the DAC. CrysAlis (Oxford Diffraction 2006) and other softwares may also be used for integration and scaling purpose and considered for the future.

As the available number of reflections from a single-crystal was limited by its DAC opening, data from six individual grains have been used to determine the space group of seifertite at 129 GPa. Observed systematically absent reflections allowed only space group: *Pbcn* (no. 60), confirming the prediction by theory (Karki et al. 1997a, 1997b; Teter et al. 1998). The same six grains were selected for structure solution and refinement. Pole figures shown in Figure 3 represent the random crystallographic orientations of six selected grains. Compatibility between these six data sets has been checked by merging them using the XSCALE software available within the XDS package. In total 613 reflections have been combined providing a redundancy of 6.6. Ten misfits due to overlap of reflections from different grains, overlap with diamond peaks, or locations close to shaded areas have been rejected by XDS automatically. Data completeness of 92.1% was achieved in the *d*-spacing range down to 0.72 Å, approaching nearly full access to a reflection sphere of the structure. The position of Si was determined from a Patterson map, and coordinates of O were obtained from a difference electron density map calculated after refinement of the Si atomic position. The refinement of the structure was performed against the resulting intensity data of 81 independent reflections using anisotropic thermal parameters. Ten independent reflections were not included into the refinement, but used to calculate R_{free} value, which was not affected by overfitting. A reasonable $R_{free} = 6.4\%$ was obtained. Four misfits have been rejected from the refinement process. All the calculations were performed using the SHELX package (Sheldrick 2008). Atomic coordinates refined against all these data sets, crystallographic data, parameters of the structure refinements, and interatomic distances are given in Table 2 and are compared to the structure data from previous theoretical calculations at high pressure (Karki et al. 1997a, 1997b; Teter et al. 1998) and to the powder XRD data of the meteorite sample at ambient conditions (Dera et al. 2002). The refined structure results at 129 GPa are in good agreement with previous theoretical calculations at 120 GPa (Karki et al. 1997a, 1997b; Teter et al. 1998). However, when structures become more complicated, theory and experiment may show different strengths: as theoretical calculations can reach any pressure range, while experimental approaches may better handle complicated chemistry.

Compared with the structure of seifertite at ambient conditions in a powder meteorite sample (Dera et al. 2002), we found that compression of seifertite is nearly isotropic over the megabar pressure range with $a/c = 0.91$ and $b/c = 1.12$, a property distinct from that of low-pressure polymorphs of SiO$_2$, such as quartz (Angel et al. 1997) and stishovite (Andrault et al. 2003; Grocholski et al. 2013). The compact configuration of seifertite, especially the short distance between the neighboring unoccupied octahedral voids
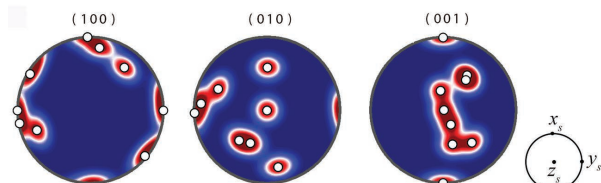
FIGURE 3. 100, 010, and 001 pole figures, representing the random orientations of six selected grains of seifertite for structure refinement. Compression axis in the DAC is along x_s and the sample was confined in a Re gasket along y_s and z_s.

TABLE 2. Atomic coordinates, crystallographic data, parameters of structure refinements, and interatomic distances in comparison with previous studies

Parameters	Multigrain This study	Theory Teter et al. (1998)	Theory Karki et al. (1997a,b)	Powder Dera et al. (2002)
P (GPa)	129	120	120	0
a (Å)	3.7277(2)	3.711	/	4.097(1)
b (Å)	4.6576(2)	4.651	/	5.0462(9)
c (Å)	4.1609(3)	4.159	/	4.4946(8)
xSi	0	0	0	0
ySi	0.1504(3)	0.1502	0.1501	0.1522(9)
zSi	0.25	0.25	0.25	0.25
xO	0.7418(4)	0.7424	0.7423	0.7336(19)
yO	0.6130(3)	0.6130	0.6134	0.6245(12)
zO	0.919(1)	0.9201	0.9201	0.9186(29)
U_{eq}-Si	0.0067(7)	/	/	0.01
U_{eq}-O	0.0069(8)	/	/	0.001
Measured/independent/free reflections	609/81/10	/	/	/
Refined parameters	15	/	/	/
R/R_{free}	0.056/0.064	/	/	/
R_{int}	0.096	/	/	0.034
Completeness	92.1%	/	/	/
Redundancy	6.6	/	/	/
Si-O	1.624(2) ×2	1.621 ×2	/	1.735 ×2
Si-O	1.655(3) ×2	1.650 ×2	/	1.783 ×2
Si-O	1.677(2) ×2	1.676 ×2	/	1.861 ×2

(Dera et al. 2002), may contribute to such behavior.

In this study, the FABLE and XDS packages were bridged to determine the structure of a minor phase in a polycrystalline mineral assemblage contained in a DAC. This study demonstrates that the multigrain approach (Sørensen et al. 2012) can be applied to tough data collections for studying phase transitions, crystal chemistry, and chemical reactions in a petrological multiphase system under P-T conditions representative of the deep Earth.

REFERENCES CITED

Andrault, D., Angel, R.J., Mosenfelder, J.L., and Le Bihan, T. (2003) Equation of state of stishovite to lower mantle pressures. American Mineralogist, 88, 301–307.
Andrault, D., Pesce, G., Bouhifd, M.A., Bolfan-Casanova, N., Henot, J.M., and Mezouar, M. (2014) Melting of subducted basalt at the core-mantle boundary. Science, 344, 892–895.
Angel, R.J., Allan, D.R., Miletich, R., and Finger, L.W. (1997) The use of quartz as an internal pressure standard in high-pressure crystallography. Journal of Applied Crystallography, 30, 461–466.
Belonoshko, A.B., Dubrovinsky, L.S., and Dubrovinsky, N.A. (1996) A new high-pressure silica phase obtained by molecular dynamics. American Mineralogist, 81, 785–788.
Boehler, R. (2006) New diamond cell for single-crystal X-ray diffraction. Review of Scientific Instruments, 77(11), 115103.
Busing, W.R., and Levy, H.A. (1967) Angle calculations for 3- and 4-circle X-ray and neutron diffractometers. Acta Crystallographica, 22, 457–464.
Cohen, R.E. (1992) First-principles predictions of elasticity and phase transitions in high pressure SiO$_2$ and geophysical implications. In Y. Syono and M.H. Manghnani, Eds., High-Pressure Research: Application to Earth and Planetary Sciences. American Geophysical Union, Washington, D.C.
Dera, P., Prewitt, C.T., Boctor, N.Z., and Hemley, R.J. (2002) Characterization of a high-pressure phase of silica from the Martian meteorite Shergotty. American Mineralogist, 87, 1018–1023.
Dubrovinsky, L.S., Saxena, S.K., Lazor, P., Ahuja, R., Eriksson, O., Wills, J.M., and Johansson, B. (1997) Experimental and theoretical indentification of a new high pressure phase of silica. Nature, 388, 362–365.
El Goresy, A., Dera, P., Sharp, T.G., Prewitt, C.T., Chen, M., Dubrovinsky, L., Wopenka, B., Boctor, N.Z., and Hemley, R.J. (2008) Seifertite, a dense orthorhombic polymorph of silica from the Martian meteorites Shergotty and Zagami. European Journal of Mineralogy, 20, 523–528.
Fei, Y., Ricolleau, A., Frank, M., Mibe, K., Shen, G., and Prakapenka, V. (2007) Toward an internally consistent pressure scale. Proceedings of the National Academy of Sciences, 104, 9182–9186.
Grocholski, B., Shim, S.H., and Prakapenka, V.B. (2013) Stability, metastability, and elastic properties of a dense silica polymorph, seifertite. Journal of Geophysical Research: Solid Earth, 118(9), 4745–4757.
Hirose, K., Takafuji, N., Sata, N., and Ohishi, Y. (2005) Phase transition and density of subducted MORB crust in the lower mantle. Earth and Planetary Science Letters, 237(1-2), 239–251.
Holland, T.J.B., and Redfern, S.A.T. (1997) Unit cell refinement from powder diffraction data: the use of regression diagnostics. Mineralogical Magazine, 61, 65–77.
Kabsch, W. (2010) XDS. Acta Crystallographica, D66, 125–132.
Karki, B.B., Warren, M.C., Stixrude, L., Ackland, G.J., and Crain, J. (1997a) Ab initio studies of high-pressure structural transformations in silica. Physical Review B, 55(6), 3465–3471.
——— (1997b) Erratum: Ab initio studies of high-pressure structural transformations in silica. Physical Review B, 56(5), 2884.
Kingma, K.J., Cohen, R.E., Hemley, R.J., and Mao, H.-K. (1994) Transformation of stishovite to a denser phase at lower-mantle pressures. Nature, 374, 243–245.
Miletich, R., Allan, D.R., and Kuhs, W.F. (2000) High-pressure single-crystal techniques. Reviews in Mineralogy and Geochemistry, 41(1), 445–519.
Murakami, M. (2003) Stability of CaCl$_2$-type and α-PbO$_2$-type SiO$_2$ at high pressure and temperature determined by in-situ X-ray measurements. Geophysical Research Letters, 30(5), 1207.
Nisr, C., Ribárik, G., Ungár, T., Vaughan, G.B.M., Cordier, P., and Merkel, S. (2012) High-resolution three-dimensional X-ray diffraction study of dislocations in grains of MgGeO$_3$ post-perovskite at 90 GPa. Journal of Geophysical Research: Solid Earth, 117(B3), B03201.
Oxford Diffraction (2006) CrysAlis Red. Oxford Diffraction, Abingdon, Oxfordshire, England.
Schmidt, S. (2014) GrainSpotter: a fast and robust polycrystalline indexing algorithm. Journal of Applied Crystallography, 47(1), 276–284.
Sharp, T.G., El Goresy, A., Wopenka, B., and Chen, M. (1999) A post-stishovite SiO$_2$ polymorph in the meteorite Shergotty: Implications for impact events. Science, 284, 1511–1513.
Sheldrick, G.M. (2008) A short history of SHELX. Acta Crystallographica A, 64, 112–122.
Sørensen, H.O., Schmidt, S., Wright, J.P., Vaughan, G.B.M., Techert, S., Garman, E.F., Oddershede, J., Davaasambuu, J., Paithankar, K.S., Gundlach, C., and Poulsen, H.F. (2012) Multigrain crystallography. Zeitschrift für Kristallographie, 227(1), 63–78.
Teter, D.M., Hemley, R.J., Kresse, G., and Hafner, J. (1998) High pressure polymorphism in silica. Physical Review Letters, 80(10), 2145–2148.
Tse, J., Klug, D., and Le Page, Y. (1992) Novel high pressure phase of silica. Physical Review Letters, 69(25), 3647–3649.
Tsuchida, Y., and Yagi, T. (1990) New pressure-induced transformations of silica at room temperature. Nature, 347, 267–269.
Zhang, L., Meng, Y., Dera, P., Yang, W., Mao, W.L., and Mao, H.K. (2013) Single-crystal structure determination of (Mg,Fe)SiO$_3$ postperovskite. Proceedings of the National Academy of Sciences, 110, 6292–6295.
Zhang, L., Meng, Y., Yang, W., Wang, L., Mao, W.L., Zeng, Q.S., Jeong, J.S., Wagner, A.J., Mkhoyan, K.A., Liu, W., Xu, R., and Mao, H.K. (2014) Disproportionation of (Mg,Fe)SiO$_3$ perovskite in Earth's deep lower mantle. Science, 344, 877–882.